Structural changes of vanadium–molybdenum–tungsten mixed oxide catalysts during the selective oxidation of acrolein to acrylic acid

Lars Giebeler [a,*], Philip Kampe [b,**], Andreas Wirth [a], Andreas H. Adams [a], Jan Kunert [b], Hartmut Fuess [a], Herbert Vogel [b]

[a] *Darmstadt University of Technology, Department of Materials Sciences, Structure Research, Petersenstr. 23, D-64287 Darmstadt, Germany*
[b] *Darmstadt University of Technology, Department of Chemistry, Ernst-Berl-Institute of Chemical Engineering and Macromolecular Science, Petersenstr. 20, D-64287 Darmstadt, Germany*

Abstract

The catalytic performance of vanadium–molybdenum–tungsten mixed oxides with the basic composition $V_2Mo_8W_xO_y$ with $0 \leq x \leq 5$ and their structural changes were examined by TPR and XRD. The variation of the tungsten content in the vanadium–molybdenum oxide matrix allowed the study of structural and catalytic performances under laboratory conditions in a downscaled version of the complex industrial catalyst.

Focussing the influence of morphology and tungsten doping on the redox properties and the oxygen dynamics, TPR experiments revealed a strong impact of the preparation method on the catalytic activity. A higher selectivity towards acrylic acid with increasing tungsten content was detected. Parallel to this, a shift of the selectivity maximum to higher temperatures was found. For the spray-dried samples, an increasing yield of acrylic acid was observed while the yield of the crystallized samples remained constant. The conversion of acrolein changed to the total oxidation products at above 450 °C. Additional cyclic temperature programmed experiments were carried out to examine the start-up behavior of the calcined catalysts under transient conditions. These experiments give also an indication of the catalysts' stability.

The structural changes of the samples were examined by Rietveld refinements of X-ray data. For the solid-state prepared samples only thermodynamically stable phases like orthorhombic MoO_3 or V_2MoO_8 were detected. $Mo_{0.6}W_{0.4}O_3$ and $Mo_{0.29}W_{0.71}O_3$ were observed at increasing tungsten content. The wet chemically prepared samples showed thermodynamically metastable phase compositions like hexagonal $(V,Mo)O_3$ and triclinic $(V,Mo)_2O_5$. Amorphous to nanocrystalline diffraction pattern are characteristic for the spray-dried samples with a tungsten content $x > 1$. A complete switch of the phase system after reduction was observed for lower tungsten contents. Only binary oxides like MoO_2 or VO_2 were measured. A destruction of the phase systems depending on the gas phase composition was observed from 450 °C on by *in situ* X-ray diffraction.
© 2006 Elsevier B.V. All rights reserved.

Keywords: Acrolein; Acrylic acid; Molybdenum; Selective oxidation catalysis; Temperature programmed reduction; Tungsten; Vanadium; XRD

1. Introduction

The production of acrylic acid increased from only 400.000 tons per year in 1980 [1] to more than 2 million tons in 2004 [2]. (Poly)acrylic acid is mainly used for superabsorbing materials, disposable diaspers and low-phosphorous detergents. Vanadium–molybdenum mixed oxide catalysts are applied in the industrial production. Different elements (e.g. Mn, Fe, Cu, W) are added as promoters in order to improve the selectivity

of the oxidation reaction of acrolein to acrylic acid [1] and the long-term stability of the catalyst. Some of them, e.g. copper [3] and tungsten [4] modify the acid-base properties of the surface and consequently the heat of adsorption [5,6].

The detailed mechanism, the structure and structural modifications of the catalyst have extensively been studied in the past. The main results obtained by EPR, IR, XPS, XRD, catalytic and sorption experiments were published in two review articles [5,6]. Bulk oxide material as well as supported catalysts on high-surface-area SiO_2 [5] were examined for their phase composition, active centers and catalytic activity [5,6]. A major influence of the support was experimentally excluded [7], the active phases and centers should be identical for bulk oxides and supported catalysts. In material with a V_2O_4 content up to

* Corresponding author. Tel.: +49 6151 166355; fax: +49 6151 166023.
** Co-corresponding author. Tel.: +49 6151 162426; fax: +49 6151 163465.
E-mail addresses: giebeler@st.tu-darmstadt.de (L. Giebeler), kampe@ct.chemie.tu-darmstadt.de (P. Kampe).

3 mol.% the compound VMo_3O_{11+x} was identified as the most active phase whereas for higher V_2O_4 contents other phases as VMo_2O_{8+x}, $V_6Mo_4O_{25}$ or V_2MoO_8 were formed. These materials exhibit lower selectivity than VMo_3O_{11+x} for acrylic acid in this order which decreased parallel to an increase of the V(V) content and parallel to a considerable shift to total oxidation products [5].

The reaction of acrolein to acrylic acid is accompanied by a fast deactivation of the material under technical conditions for bulk vanadium–molybdenum mixed oxides. This operation mode results in thermodynamically stable phases like orthorhombic MoO_3 and monoclinic V_2MoO_8 which are inactive towards the formation of acrylic acid as shown by solid-state prepared samples [8].

In the copper-modified vanadium–molybdenum oxide catalysts the active phase was reported as VMo_3O_{11+x} and VMo_2O_{8+x} where vanadium is partially substituted by variable amounts of copper [3]. For catalysts with tungsten as promoter, Mo_5O_{14} is suggested as active phase with variable but minor contents of vanadium and tungsten [4].

Both oxides, Mo_4O_{11} and Mo_5O_{14} with partial substitution of vanadium and tungsten for molybdenum, build layer structures which, by integration or removal of oxygen, may form shear structures.

In order to deepen the knowledge of the active sites and oxygen transfer in these catalytic systems, mixed oxides were prepared differently and examined by nitrogen adsorption (BET model), X-ray diffraction (XRD) and temperature programmed reduction with acrolein (TPR).

2. Experimental

2.1. Preparation

The preparation of catalysts with the formal composition $V_2Mo_8W_xO_y$ ($0 \leq x \leq 5$) was performed via two different ways

(Table 1). The first oxide series I was prepared by melting and calcination of the binary oxides MoO_3, V_2O_5 and WO_3 in the desired stoichiometry to obtain oxides with thermodynamically stable phases. Therefore, the oxides were homogenized in an agate mortar and melted in a sealed vacuum quartz tube. Then the powder was pressed into pellets and was annealed in a muffle furnace for seven days at 600 °C. After the calcination procedure the pellets were quenched in liquid nitrogen to stabilize the formed crystalline phases.

The second method of preparation is based on aqueous solutions of the ammonium salts acidified with nitric acid. To prepare the oxides, the precursor solutions were dried via crystallization (IIa) and spray-drying (IIb). The obtained powder was treated in a special furnace with an annealing program up to 400 °C as temperature maximum. The details of preparation (I) can be found in Adams et al. [8] and the preparation of the oxides through aqueous solutions (IIa and IIb) in Kunert et al. [9].

2.2. Temperature programmed reduction

The performance of the catalysts was characterized by TPR in a micro reactor with acrolein as reducing agent. The design of the TPR equipment was published by Boehling et al. [10]. The reaction products were analyzed by a quadrupole mass spectrometer (Balzers, QMG 511). A continuous analysis of acrolein, acrylic acid, carbon dioxide, carbon monoxide and water was achieved through online monitoring.

Two hundred fifty milligrams of a probe was pre-treated at 400 °C for 60 min with 10 vol.% oxygen (Messer Griesheim) in inert gas with a flow rate of 1.2 l/h and subsequently cooled down to room temperature in inert gas. An inert gas mixture, argon with 5 vol.% helium (Messer Griesheim) as internal standard for the MS analysis was applied. The reduction was carried out with 5 vol.% acrolein (BASF) in the standard inert gas mixture Ar/He. The temperature was raised with a constant heating rate of 10 °C min^{-1} to a maximum of 480 °C and cooled down to

Table 1
Observed structure types for the samples of preparation methods I, IIa and IIb before and after TPR

Structure types	Preparation method		I	IIa		IIb	
	SG	Reference		Before	After	Before	After
VO_2	$P2_1/c$	[21]		X[a]			
VO_2	$C2/m$	[25]			X		X
$(V,Mo)O_3$	$P6_3$	[18]		X		X	
$(V,Mo)_2O_5$	$P1$	[19]		X		X	
V_2MoO_8	$C2/m$	[15]	X				
MoO_2	$P2_1$	[24]			X		X
MoO_3	$Pnma$	[14]	X				
MoO_3	$Pbnm$	[26,28]			X	X[b]	X[c]
MoO_3	$P2_1/c$	[27]			X		
Mo_5O_{14}	$P2_1/a$	[22]		X[a]	X[a]		
Mo_5O_{14}	$P4/mbm$	[29]				X[b]	X[c]
$Mo_{0.6}W_{0.4}O_3$	$Cmc2_1$	[16]	X				
$Mo_{0.29}W_{0.71}O_3$	$P2_1/n$	[16]	X				
WO_3	$P6/mmm$	[20]		X[a]	X		X

[a] Only $x = 3$.
[b] $x > 1$ nanocrystalline/amorphous.
[c] $x > 2$ nanocrystalline/amorphous.

400 °C followed by a re-oxidation of the catalyst under the conditions of the pre-treatment. At least two reduction/re-oxidation cycles were performed. No re-oxidation was performed after the second reduction cycle. The contour plots for selectivity, conversion and yield were calculated from the gas phase analysis. The values for the mixed oxides with tungsten contents $x = 2.5$, 3.5 and 4.5 were approximated by a mathematical 2-point or 3-point interpolation which does not lead to a shortening of the plots but to a better clarity and interpretability.

2.3. X-ray diffraction

The powder samples were fixed as a thin layer on an acetate film. X-ray diffraction data were collected on a STOE STADI-P powder diffractometer by Mo K α1-radiation ($\lambda = 0.70926$ Å) and a position sensitive detector (PSD) in the range of $3° \leq 2\theta \leq 40°$. Additional data were measured by Cu K α1-radiation ($\lambda = 1.54051$ Å) in the range of $5° \leq 2\theta \leq 80°$. In both cases the measurements were performed in transmission geometry with a Ge (1 1 1) monochromator and a step size $\Delta 2\theta = 0.02°$. Structure refinements were carried out with FullProf [11] in the program package WinPLOTR according to the Rietveld method [12].

For the *in situ* X-ray diffraction measurements a high-temperature chamber HDK 2.4 (Johanna Otto GmbH) was used in combination with a Siemens D500 (Cu K α1 radiation, pyrolytic graphite secondary monochromator, scintillation detector). The samples were measured for 15–30 h at 300, 400 and 500 °C in the range of $5° < 2\theta < 80°$ and a step size of $\Delta 2\theta = 0.03°$ in Bragg–Brentano geometry with a defined oxygen partial pressure ($p(O_2) = 21\%$ and 0.03%).

2.4. Adsorption studies (BET)

The specific surface area was determined by the BET method. Before the measurements the samples were dried at 80 °C at 10 Pa for 20 h. For the measurement of the specific BET surface area (S_{BET}), nitrogen was adsorbed at -196 °C on 0.3–0.6 g powder. For the automatic data logging and evaluation, a Quantachrome Autosorb 3B was used. The specific surface S_{BET} of the samples prepared by I was about 1–2 m^2 g^{-1} and for the samples prepared by IIa and IIb in the range of 3–15 m^2 g^{-1}.

No influence of the tungsten content on the S_{BET} was observed. The preparation method itself leads to the higher S_{BET} of the wet chemical prepared samples (II) but the specific surface seems to have only a negligible effect on catalysis.

3. Results and discussion

3.1. In situ characterization by temperature programmed reduction

3.1.1. Influence of tungsten doping and the preparation method

The influence of the preparation method as well as the gradual doping with tungsten on the catalytic performance of the mixed oxides ($V_2Mo_8W_xO_y$ with $0 \leq x \leq 5$) was investigated.
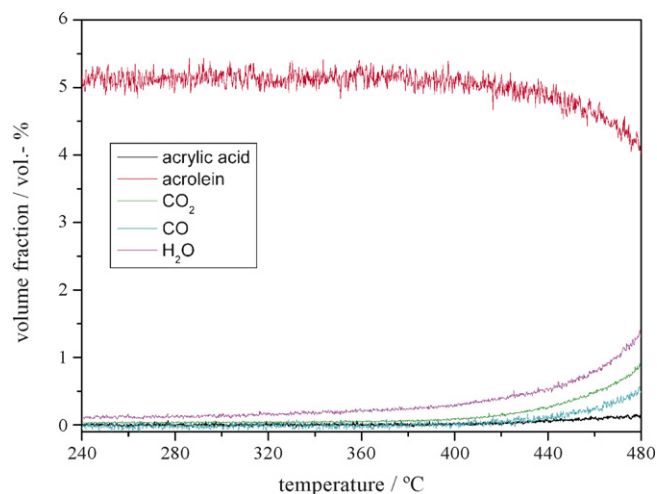

Fig. 1. Profile of the temperature programmed reduction of $V_2Mo_8O_y$, prepared via solid phase reaction, with acrolein in inert gas as reducing agent (heating rate: 10 °C min^{-1}).

Both samples IIa (crystallized) and IIb (spray-dried) were examined in detail. The samples of method I are only used to compare the phase compositions with that of the samples prepared by IIa and IIb. As reported for binary vanadium–molybdenum mixed oxides prepared by method I no reduction was indicated in the investigated temperature region [8]. Samples I hardly show any catalytic activity towards acrylic acid formation as is exemplarily indicated by the concentration profile in dependence on time for the sample $V_2Mo_8O_y$ (Fig. 1). Conversion of acrolein begins only above 400 °C where basically the total oxidation products are formed. Based on this observation and the stabilization of vanadium–molybdenum oxides by tungsten, no fundamentally new information can be expected from TPR in the investigated temperature region for the samples prepared by melting process (samples I). So we decided to pass on TPR measurement of method I samples.

The results of the TPR experiments in terms of activity and selectivity are presented in Figs. 2–4 for the samples IIa and IIb as a function of temperature and tungsten content. Particularly, the second reduction cycle is chosen because here the start-up phase is completed (q.v. 3.1.2). A strong influence of the preparation method on the selectivity to acrylic acid is obvious especially for tungsten contents $x > 2$. The samples IIb (Fig. 2b) show consistently higher selectivities than IIa (Fig. 2a). The selectivity of IIb reaches a maximum of 91% around 350 °C for a tungsten content $3 \leq x \leq 4$. With an increasing amount of tungsten the maximum of selectivity shifts to higher temperatures (from 270 to 350 °C) accompanied by higher absolute values. The samples IIa reach a maximum in selectivity of only 70% at 250 °C and a tungsten content of $x = 0.5$ (Fig. 2a). Selectivity decreases with rising temperature due to the total oxidation reactions and reaches a value near zero above 470 °C. Thus, with higher tungsten content an increase in selectivity is most pronounced for the samples IIb.

Activity is discussed taking into account only the temperature range below 450 °C in which selective oxidation is dominant.
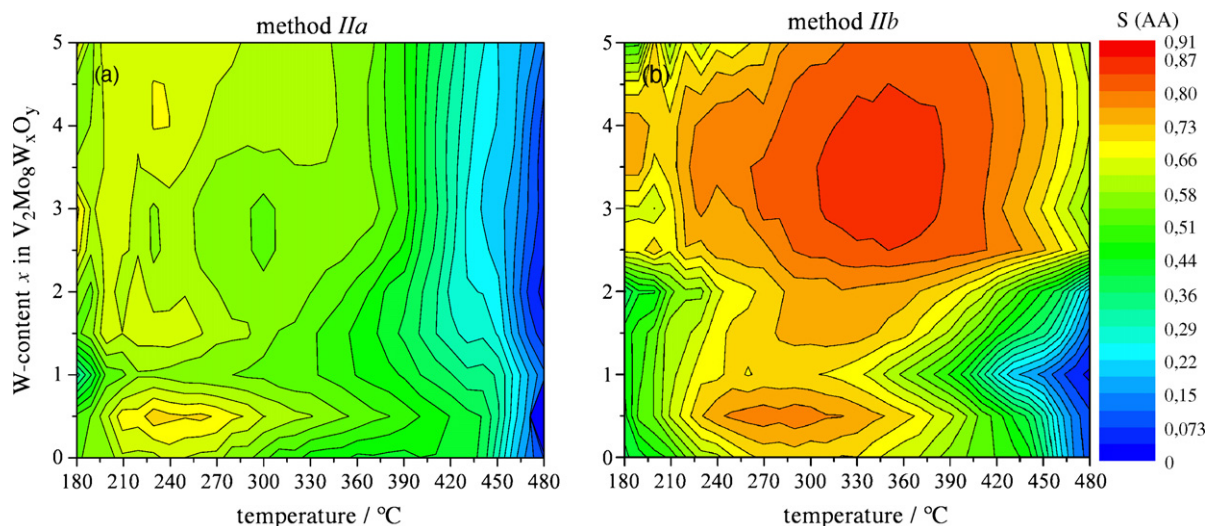
Fig. 2. Selectivity to acrylic acid, 2nd TPR cycle with 5 vol.% acrolein, heating rate 10 °C min^{-1}, plotted are all mixed oxides of the W-variation x (V$_2$Mo$_8$W$_x$O$_y$). 2a (left): method IIa, 2b (right): method IIb catalysts.

Above 450 °C the total oxidation becomes dominant as demonstrated by the selectivity plot (Fig. 2). The catalytic activity of samples IIb (Fig. 3b) shifts with increasing tungsten content to higher temperatures and conversion also increases. The samples of IIa show only very little sensitivity to the tungsten content (Fig. 3a). The samples of IIa activate acrolein from 190 °C on while the catalysts of IIb only become active above 200–240 °C depending on the tungsten content. Even the absolute values are slightly higher for the catalysts of method IIa. Thus, the positive influence of spray-drying on the selectivity is accompanied with a slight drawback in activity. In general, the addition of tungsten increases the activity of both preparation routes. According to the same trends in activity and selectivity, the maximum yield of acrylic acid shifts from 320 °C (10%) to 360 °C (13%) for

the series IIb (Fig. 4b). Catalysts of IIa reach a maximum yield of only 8% at 330 °C (Fig. 4a). The origin of the calculated yields from TPR should be emphasized. Hence, oxidation takes place only with solid-state oxygen. In the presence of gas phase oxygen, the selectivity and therewith the yield of acrylic acid at temperatures higher than 380 °C would decrease significantly due to gas phase oxidation.

3.1.2. The start-up phase

As described in chapter 2.2, cyclic temperature programmed reductions and re-oxidations were run. Hence, the samples IIa and IIb in the above described second reduction cycle exhibit a thermal and catalytic history leading to changes in structure and performance compared to the calcined samples. These changes
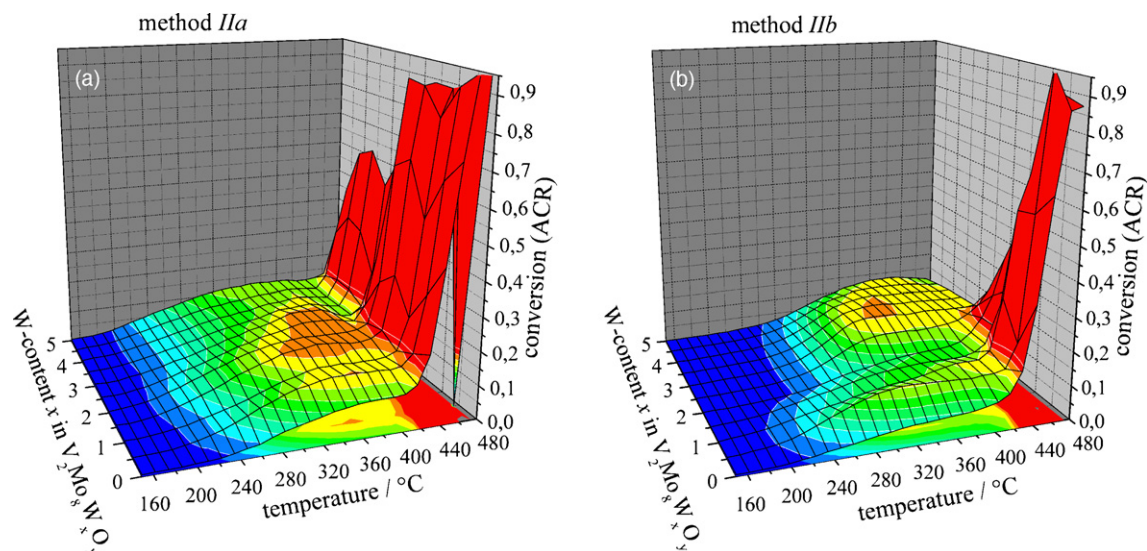

Fig. 3. Conversion of acrolein, 2nd TPR cycle with 5 vol.% acrolein, heating rate 10 °C min^{-1}, plotted are all mixed oxides of the W-variation x (V$_2$Mo$_8$W$_x$O$_y$). 3a (left): method IIa, 3b (right): method IIb catalysts.
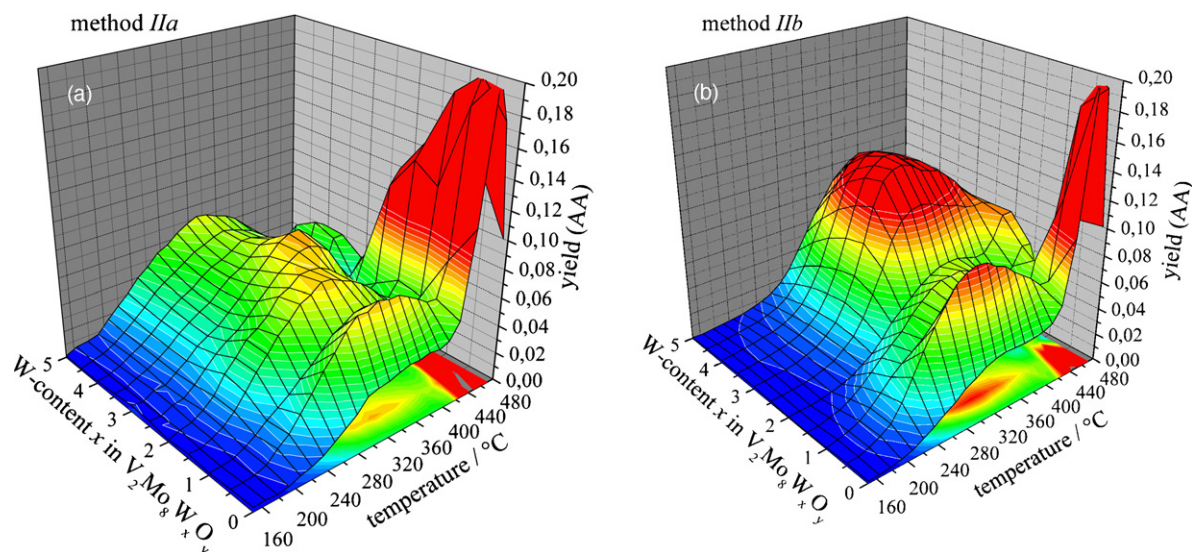
Fig. 4. Yield of acrylic acid, 2nd TPR cycle with 5 vol.% acrolein, heating rate $10\,°C\,min^{-1}$, plotted are all mixed oxides of the W-variation x ($V_2Mo_8W_xO_y$). 4a (left): method IIa, 4b (right): method IIb catalysts.

under different reaction gas conditions are commonly described as start-up phase. Usually the start-up phase is completed only after several days. In order to accelerate this process, the applied temperature program up to 480 °C reaches the thermal stability limit of the mixed oxides.

In Fig. 5a and b, the absolute conversion values of the first reduction cycle are subtracted from the values of the second cycle (Fig. 3) which leads to a difference plot showing the changes throughout the start-up phase. Negative areas indicate higher conversion in the first cycle while positive areas would state that the activity in the first cycle did not reach the activity of the second one. In the latter case, the start-up process would have activated the catalyst. The change of the colors from blue to red comes up to the change from negative to positive values.

The minor tungsten doped samples IIa show an increasing activity while the samples with a tungsten content $x \geq 3$ show hardly any changes in activity. The only exception is the deactivation of the sample with a tungsten content $x = 5$ (Fig. 5a). As demonstrated by the X-ray pattern this catalyst has undergone a re-crystallization process (Figs. 8 and 9).

The samples IIb can be divided into three groups. Mixed oxides with a tungsten content $x < 1$ are slightly activating (Fig. 5b). Samples with $1 \leq x \leq 2$ are shown by XRD to re-crystallize during the start-up phase accompanied by a deactivation (Figs. 10 and 11). Samples with $x > 2$ remain more or less constant in activity. The XRD pattern demonstrated a high degree of amorphous material for this composition. This is again a proof of the positive influence of amorphous catalysts on the activity.
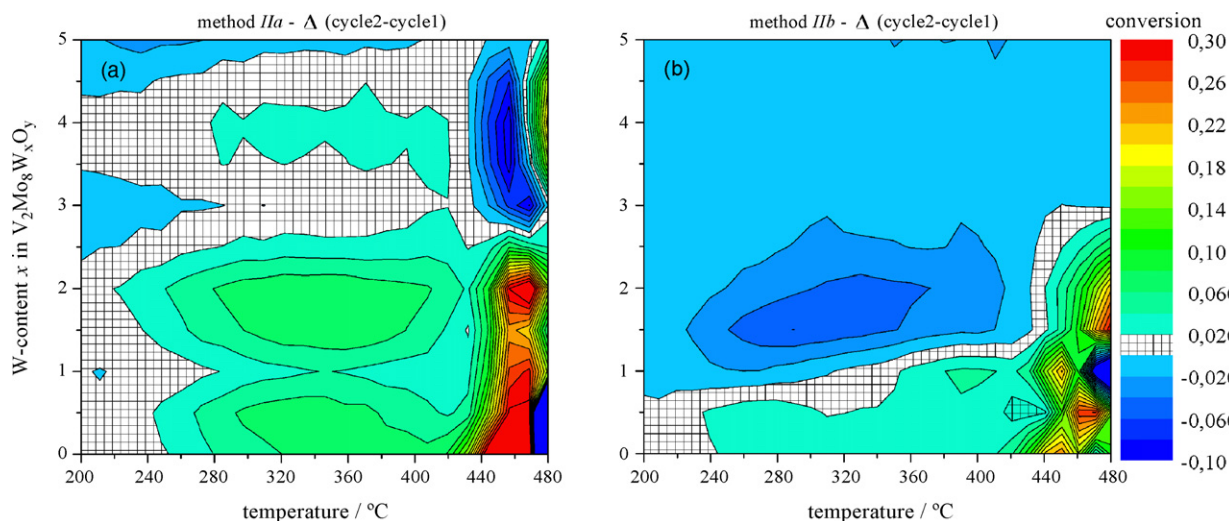

Fig. 5. Difference plot of conversion of acrolein, 2nd TPR cycle – 1st TPR cycle, 5 vol.% acrolein, heating rate $10\,°C\,min^{-1}$, plotted are all mixed oxides of the W-variation x ($V_2Mo_8W_xO_y$). 5a (left): method IIa, 5b (right): method IIb catalysts.
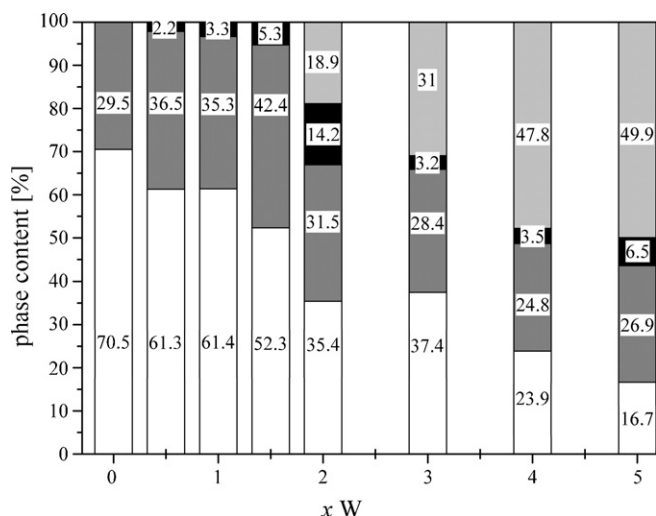
Fig. 6. Crystalline phases in $V_2Mo_8W_xO_y$ mixed oxides prepared by method I ($0 \leq x \leq 5$). (□) MoO_3, (▨) V_2MoO_8, (■) $Mo_{0.6}W_{0.4}O_3$, (▧) $Mo_{0.29}W_{0.71}O_3$.

Within the start-up phase the activity behavior of samples IIa and IIb converges. The comparison of the X-ray pattern shows the same behavior for the whole phase composition. Based on the evidence of TPR and XRD it is concluded that only high tungsten contents ($x > 2$) prevent the mixed oxides from this re-crystallization process. From the second TPR cycle on, the reduction behavior of the mixed oxides is reproducible and constant.

3.2. Phase composition

The various materials were examined in detail by X-ray powder diffraction after preparation and after the TPR experiments. The phases are determined by Rietveld refinement and are compiled in Table 1.

3.2.1. Samples prepared by method I

The material prepared by method I with the general stoichiometry $V_2Mo_8W_xO_y$ ($0 \leq x \leq 5$) (Fig. 6) exhibits similar phases as described in the phase diagram of Volkov et al. [13] for the system V_2O_5–MoO_3. Especially the phases V_2MoO_8 and MoO_3 are present. The existence of V_2MoO_8 and MoO_3 may be classified as a criterion for a thermodynamic equilibrium and the existence of thermodynamically stable phases [6]. At increasing tungsten content ($x > 0$) two additional molybdenum–tungsten oxide phases are found.

The Rietveld refinement was based on the structure models of MoO_3, SG *Pnma* [14] and V_2MoO_8 with SG *C2/m* [15]. MoO_3 shows a layer structure which is built of chains of staggered edge-sharing MoO_6 octahedra. The V_2MoO_8 structure can be described as a shear structure of octahedra forming ReO_3 layers. Only in *a* direction a short range order of three layers of octahedra is arranged by common edges. At a tungsten content $x = 0$ these two models are sufficient to interpret the X-ray pattern. In the range of $0.5 \leq x \leq 1.5$ a phase refined with the structure of $Mo_{0.6}W_{0.4}O_3$, SG *Cmc2₁* [16], is detected. Between $2 \leq x \leq 5$,

a fourth phase refined with $Mo_{0.29}W_{0.71}O_3$, SG *P 2₁/n* [16] as structure model, is observed (Fig. 6). Both structures consist of a three-dimensional network of corner-linked octahedra. Differences are a distortion of the octahedra in $Mo_{0.6}W_{0.4}O_3$ and the tilted octahedra in $Mo_{0.29}W_{0.71}O_3$.

As mentioned above MoO_3 and V_2MoO_8 are the thermodynamically stable oxides for the V_2O_5–MoO_3 system at 600 °C [13] and the $Mo_{0.6}W_{0.4}O_3$ is a thermodynamically stable oxide in the MoO_3–WO_3 phase diagram at 600 °C [16]. The $Mo_{0.29}W_{0.71}O_3$, stable between 150 and 340 °C, is a result of a fast phase transformation of an orthorhombic WO_3, *SG Pnmb*, stable at 600 °C [16] during cooling before quenching and a subsequent fixing of the phase composition. In conclusion two oxidic systems are found. The described compounds seem to be mixed oxides even with solid-state preparation. Admittedly an embedding of vanadium cations into the molybdenum tungsten oxides has to be assumed because of the tolerance of tungsten and of course molybdenum oxide structures for extrinsic cations. This circumstance has also to be viewed for crystal structures determined by the phase diagrams of Volkov et al. for V_2O_5–MoO_3 and for V_2O_5–WO_3 by Freundlich [17] in the special cases of vanadium-substitution in the system V_2O_5–MoO_3 and V_2O_5–WO_3.

3.2.2. Catalysts before and after reduction prepared by method IIa

The samples before activation and reaction are composed of phases with the structure types of hexagonal $(V,Mo)O_3$, SG *P 6₃* [18], and triclinic $(V,Mo)_2O_5$, SG *P 1* [19] as shown in Fig. 7a. With increasing tungsten content a structure with a hexagonal WO_3 type, SG *P 6/mmm* [20], is observed (Fig. 8). The increase of the tungsten dominated phase results in the decrease of the vanadium–molybdenum oxide phases. An exception is the sample with a tungsten content $x = 3$. It is characterized by a different phase composition because of the non-perfect decomposition of the ammonium molybdate educt during calcination. The irrelevance of this circumstance is shown by TPR and XRD after reduction. The X-ray pattern is refined by a hexagonal WO_3 structure type, SG *P6/mmm* [20], and monoclinic VO_2, SG *P2₁/c* [21], monoclinic Mo_5O_{14}, SG *P2₁/a* [22] as well as a triclinic $(NH_4)_2Mo_4O_{13}$, SG *P -1* [23]. The phase contents of $x = 5$ are approximated because of the amorphous characteristic of the X-ray pattern and therefore the quality loss at refinement.

After reduction with acrolein a complete conversion of the phase system can be observed. As shown in Fig. 7b, monoclinic MoO_2, SG *P2₁* [24], monoclinic VO_2, SG *C2/m* [25], and in some cases hexagonal WO_3, SG *P6/mmm* [20], and orthorhombic MoO_3, SG *Pbnm* [26], or monoclinic MoO_3, SG *P2₁/c* [27] are the main components. Additionally at the tungsten content $x = 3$ monoclinic Mo_5O_{14}, SG *P2₁/a* [22], is found (Fig. 9).

3.2.3. Catalysts before and after reduction prepared by method IIb

Before reaction the samples have a similar composition as shown for the ones prepared by method IIa. The Rietveld refinements (Fig. 10) were performed with phases of the structure types of hexagonal $(V,Mo)O_3$, SG *P 6₃* [18], triclinic $(V,Mo)_2O_5$
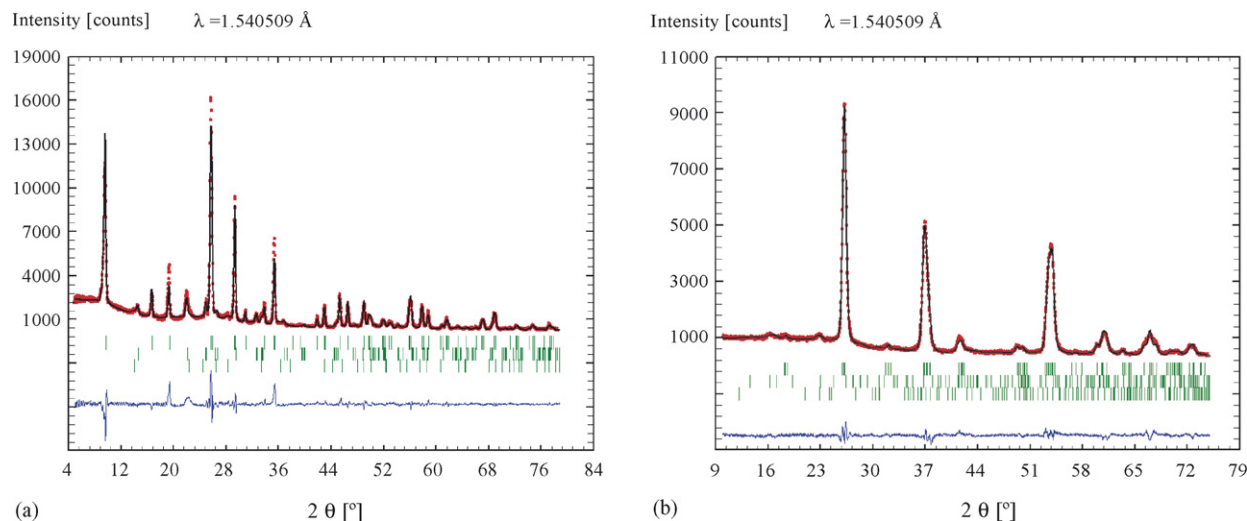
Fig. 7. (a) X-ray pattern and Rietveld refinement of $V_2Mo_8W_{0.5}O_y$ prepared by IIa before reduction. The phases from top to bottom are hexagonal $(V,Mo)O_3$, triclinic $(V,Mo)_2O_5$ and hexagonal WO_3. (b) X-ray pattern and Rietveld refinement of $V_2Mo_8W_{0.5}O_y$ prepared by IIa after reduction. The phases from top to bottom are monoclinic MoO_2, monoclinic VO_2 and monoclinic MoO_3.

structure, SG $P\,1$ [19], and hexagonal WO_3 phase, SG $P\,6/mmm$ [20]. At a tungsten content $x > 1$ the system changes completely. While the samples with tungsten contents $x \leq 1$ are well crystallized, those with $x > 1$ are amorphous with nanocrystalline particles. The sample composition consists of phases with orthorhombic MoO_3, SG $Pbnm$ [28], and tetragonal Mo_5O_{14} structure types, SG $P4/mbm$ [29], which is supported by electron diffraction.

After reduction the samples consist of phases with monoclinic MoO_2 and monoclinic VO_2 structure types. As minor phases orthorhombic MoO_3 and hexagonal WO_3 occur (Fig. 11). At tungsten contents $0 \leq x \leq 2$ these phases are detectable. Above $x > 2$, the system becomes amorphous to nanocrystalline. The phases determined are of monoclinic VO_2, orthorhombic

MoO_3 and tetragonal Mo_5O_{14} structure types. Because of the amorphous character and nanocrystallinity of the X-ray pattern the composition can only be approximated.

The results of both wet chemically prepared catalysts series show a tendency to decompose to binary oxides after reduction with occupation by a single metal only instead of mixed occupation before, e.g. the $(V,Mo)_2O_5$ structure type.

A significant trend in the structural data, e.g. lattice constants or similar, cannot be expediently established for explanation of catalytic effects. But for the ternary vanadium–molybdenum–tungsten mixed oxides the thermodynamically stable phases, in this case the phase with an orthorhombic MoO_3 structure type, seem to be more active than for the binary.
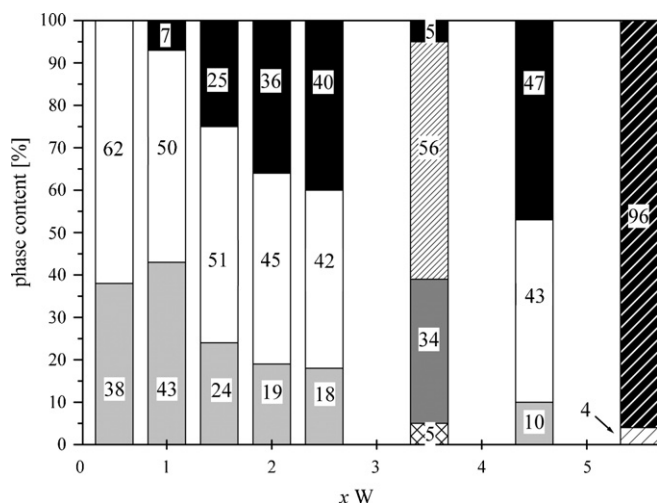

Fig. 8. Phase content of the catalyst samples $V_2Mo_8W_xO_y$ ($0 \leq x \leq 5$) prepared by IIa before reduction with acrolein. (▨) hexagonal $(V,Mo)O_3$, (□) triclinic $(V,Mo)_2O_5$, (■) hexagonal WO_3, (▨) monoclinic Mo_5O_{14}, (■) monoclinic VO_2, (⊠) triclinic $(NH_4)_2Mo_4O_{13}$, (▨) amorphous/nanocrystalline triclinic $(V,Mo)_2O_5$, (▨) amorphous/nanocrystalline hexagonal WO_3.
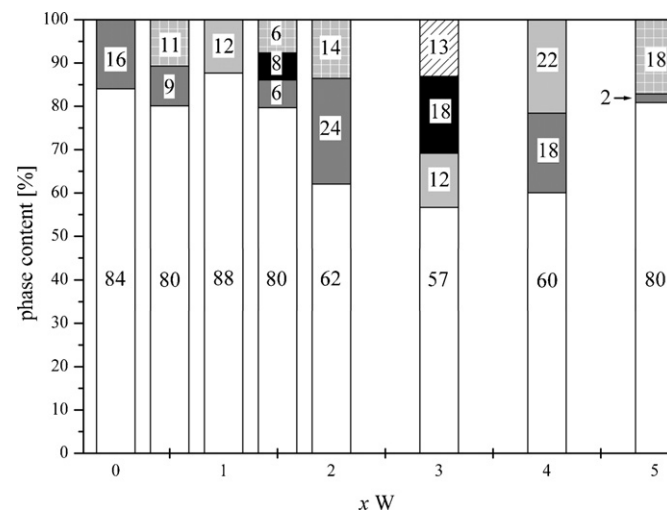

Fig. 9. Phase content of the catalyst samples $V_2Mo_8W_xO_y$ ($0 \leq x \leq 5$) prepared by IIa after reduction with acrolein. (□) monoclinic MoO_2, (■) monoclinic VO_2, (▨) orthorhombic MoO_3, (▨) monoclinic MoO_3, (■) hexagonal WO_3, (▨) monoclinic Mo_5O_{14}.
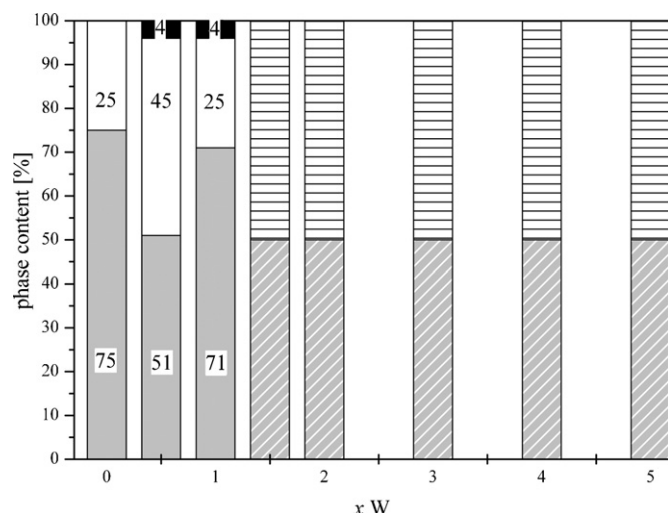
Fig. 10. Phase content of the catalyst samples $V_2Mo_8W_xO_y$ ($0 \leq x \leq 5$) prepared by IIb before reduction with acrolein. (▨) hexagonal $(VMo)O_3$, (□) triclinic $(V,Mo)_2O_5$, (■) hexagonal WO_3, (▨) amorphous/nanocrystalline orthorhombic MoO_3, (▤) amorphous/nanocrystalline tetragonal Mo_5O_{14}.

3.2.4. In situ X-ray diffraction measurements

In situ X-ray diffraction measurements at a $p(O_2) = 21\%$ (air) show a difference in stability of the samples prepared by IIa and IIb. The material prepared by IIa totally converts in 240 min at 500 °C into the thermodynamically stable phases with orthorhombic MoO_3, SG *Pbnm* [28], and monoclinic V_2MoO_8 structure types, SG *C2* [30]. Monoclinic MoO_3, SG $P2_1/c$ [27] has been detected after reduction. For the samples prepared by IIb, especially for the amorphous samples with tungsten contents $x > 1$, a longer period of conversion can be recognized [31]. Tungsten seems to stabilize especially the amorphous parts against conversion into thermodynamically stable phases. An interesting feature is the observation of the thermodynamically

Fig. 11. Phase content of the catalyst samples $V_2Mo_8W_xO_y$ ($0 \leq x \leq 5$) prepared by IIb after reduction with acrolein. (□) monoclinic MoO_2, (■) monoclinic VO_2, (▨) orthorhombic MoO_3, (■) hexagonal WO_3, (▤) amorphous/nanocrystalline tetragonal Mo_5O_{14}, (▨) amorphous/nanocrystalline monoclinic VO_2, (▨) amorphous/nanocrystalline orthorhombic MoO_3.

metastable phase with the structure type of monoclinic MoO_3. This phase is neither identified in the solid-state nor in the wet chemically prepared samples before reduction. Significant amounts are found after reduction in some of the samples prepared by IIa. The existence of phases with both MoO_3 structure types, which tolerates high concentrations of W(VI) in the lattice, and the hexagonal WO_3 structure type may play a role as reservoirs for the storage of tungsten which could not be incorporated into the MoO_2 or VO_2 structures after reduction. Under these conditions tungsten may be available for other purposes, e.g. the (re)construction of phases at re-oxidation.

At a $p(O_2) = 0.03\%$ (nitrogen) the conversion temperature shifts about 100 °C from 500 to 600 °C. At lower temperatures, no conversion can be detected on a time scale of 30 h. For the conversion of the thermodynamically metastable to the stable phases an uptake of oxygen seems to be necessary. It leads to the assumption of an existence of cations in lower oxidation states. According to investigations in the thermodynamically stable V–Mo–O system, vanadium may partially be present in lower oxidation states [19,31,32].

4. Conclusions

The examination of conversion and selectivity against temperature and tungsten content suggests that tungsten is more than a pure structure promoter especially for the samples series IIb. In contrast, no significant influence of the tungsten content is detected for the catalysts of IIa. The change in catalytic activity and selectivity can clearly be ascribed to the preparation method, the phase composition and the tungsten content especially for the samples of IIb. While tungsten has only small effects on the selectivity to acrylic acid for the crystalline samples of IIa, higher tungsten contents with $x \geq 2$ show a significant increase in selectivity for the X-ray amorphous/nanocrystalline samples of IIb. It can be related to a change in the crystal systems from a crystalline hexagonal MoO_3 and triclinic V_2O_5 system into an amorphous/nanocrystalline orthorhombic MoO_3 and tetragonal Mo_5O_{14} system. The lower selectivity for acrylic acid production and the high conversion rates of the crystalline system marks the high activity towards the total oxidation reactions. Higher selectivity as a positive influence of spray-drying (IIb) is subtended by a higher temperature for the oxidation of acrolein to acrylic acid compared to the crystallized samples (IIa). Commonly tungsten supports the increase in selectivity for both preparation methods which is close to the literature [4,33]. The activity of samples IIa and IIb converge during the start-up phase. However, this is only true for the minor doped catalysts. A higher tungsten content prevents the samples from this convergency.

The wet chemical preparation methods lead to thermodynamically metastable mixed oxides which do not exist in the phase diagrams. A total conversion to reduced phases was shown except for the samples (IIb) with tungsten contents $x > 2$. Their structures seem to be stable against reduction according to TPR and XRD. Acrolein accelerates the reduction significantly and lowers the conversion temperature as compared to the *in situ* X-ray measurements in nitrogen with low oxygen content or
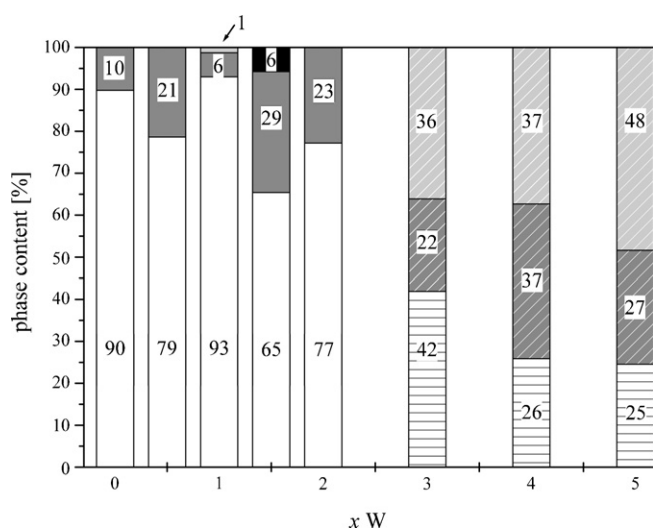
air. The thermodynamically stable phases exist in the catalytically inactive material prepared by I and the thermodynamically metastable phases in the active catalysts prepared by the wet chemical methods IIa and IIb (q.v. 3.2).

Monoclinic MoO_3 in the samples is, however, observed by treatments with acrolein and under nitrogen/oxygen mixture or air. This is explained by the stabilization of some structures by tungsten which is demonstrated by *ex situ* and *in situ* investigations. In the reduced state only small amounts of thermodynamically stable, orthorhombic MoO_3 are found. The existence of the V_2MoO_8 structure type, however, or other thermodynamically stable phases was not confirmed. So inactivity and/or deactivation of the catalysts by thermodynamically stable phases is different as compared to the ternary vanadium–molybdenum oxides [6]. A downscale from mixed-occupied metal sites and complicated structures to simple and single occupied metal sites after reduction is also started.

The reduction of MoO_3 to MoO_2 was observed during treatments with hydrogen [34,35] and propene [36] as probe molecules. The first appearance of MoO_2 was observed at $400\,^{\circ}C$ for crystalline MoO_3 in hydrogen and at $350\,^{\circ}C$ in propene containing atmosphere without any stabilization by foreign cations [35,36].

After thermal activation of V–Mo–W mixed oxides in helium [4,37] or nitrogen [38], MoO_2 was detected by Raman spectroscopy and XRD and VO_2 as a trace could not be excluded [4]. During thermal activation in the temperature range between 400 and $556\,^{\circ}C$, the catalyst material changes the structure from nanocrystalline Mo_5O_{14} structure type to crystalline and the by-products MoO_3 and MoO_2. At temperatures $\geq 550\,^{\circ}C$, the Mo_5O_{14} type oxide disproportionates into MoO_3 and MoO_2 [38]. In the case of V–Mo–W mixed oxides the temperature where MoO_2 appears first is $530\,^{\circ}C$ [38]. During acrolein oxidation in presence of oxygen neither MoO_2 nor VO_2 were detected [33]. The reaction conditions in the present work favor the formation of MoO_2 or VO_2 type oxides. In the case of the crystalline samples, no crystalline Mo_5O_{14} type oxide is observed (except IIa, $x = 3$) because the reduction temperature is much lower than the temperature of the disproportionation of the vanadium- and tungsten-doped Mo_5O_{14} to MoO_2 and MoO_3 type oxides [38]. A low background for the crystalline samples in the XRD pattern indicates only minor amorphous parts as represented by Fig. 8 and 10 with low MoO_3 and high MoO_2 contents. Thus, a direct reduction from the hexagonal MoO_3 type oxide to the MoO_2 type oxide and small amounts of MoO_3 stabilized by tungsten as by-products takes place. The same result was observed for the reduction of undoped MoO_3 [35]. This does not apply for samples of series IIb with tungsten contents $x > 2$ where only amorphous and/or nanocrystalline phases are observed. The X-ray pattern is similar compared to the one before reduction and shows the stability against reduction and therefore the disproportionation of the Mo_5O_{14} type oxide which is due to the low reaction temperature of maximum $480\,^{\circ}C$ according to literature data [38]. The trace of VO_2 may be explained by the destruction of the $(V,Mo)_2O_5$ type oxide which has not been incorporated into a molybdenum or tungsten oxide matrix.

As an alternative a reservoir function of phases with monoclinic/orthorhombic MoO_3 and hexagonal WO_3 structure types towards the storage of metal cations should be discussed, e.g. for the re-building of post-reduction phases after re-oxidation.

It can be summarized that all investigated catalysts prepared by the two different wet chemical preparation methods are more or less catalytically active and selective for acrylic acid formation at temperatures around $380\,^{\circ}C$ in TPR experiments. The increase in selectivity is directly connected to the formation of the nanocrystalline MoO_3–Mo_5O_{14} type oxide system. The high conversion rates and yields are due to the acrylic acid formation but also due to total oxidation. This circumstance is pointed out for crystalline samples at temperatures $> 400\,^{\circ}C$ where the triclinic V_2O_5 type oxide may mainly be responsible for the total oxidation. The post-reduction state for all wet chemically prepared samples consists of MoO_2 and VO_2 with hexagonal WO_3 and orthorhombic/monoclinic MoO_3 as by-products to store redundant W(VI) ions not incorporated in MoO_2 or VO_2 matrices. The samples of method IIb with tungsten contents $x > 2$ show the specific characteristic of a reduction stability in the sense of a steady-state of the structure. According to the TPR experiments tungsten increases the catalytic activity for the mixed oxides of both wet chemical preparation methods. However, the higher stability of tungsten doped mixed oxides of IIb is accompanied with a shift of activity to higher temperatures compared to the crystallized samples (IIa) with the same tungsten content. Spray-drying and the change in the crystal system lead to a higher selectivity. It hardens the assumption that tungsten is more than only a structure promoter and participates in oxidation catalysis.

Acknowledgements

References

[1] H.F. Rase, Handbook of Commercial Catalysts – Heterogeneous Catalysts, CRC Press, Boca Raton, 2000, p. 265 ff.

[2] H. Redlingshoefer, Degussa Sci. Newslett. 7 (2004) 17–19.

[3] T.G. Kuznetsova, T.V. Andrushkevich, L.M. Plyasova, V.M. Bondareva, A.A. Davydov, I.P. Olenkova, A.P. Shepelin, React. Kinet. Catal. Lett. 26 (1984) 399–403.

[4] G. Mestl, C. Linsmeier, R. Gottschall, M. Dieterle, J. Find, D. Herein, J. Jaeger, Y. Uchida, R. Schloegl, J. Mol. Catal. A 162 (2000) 463–492.

[5] T.V. Andrushkevich, Catal. Rev. Sci. Eng. 35 (1993) 213–259.

[6] J. Tichy, Appl. Catal. A 157 (1997) 363–385.

[7] N.N. Chumachenko, D.V. Tarasova, T.A. Nikoro, I.V. Yaroslavtseva, Kinet. Catal. 25 (1984) 558–560.

[8] A.H. Adams, F. Haaß, T. Buhrmester, J. Kunert, J. Ott, H. Vogel, H. Fuess, J. Mol. Catal. A 216 (2004) 67–74.

[9] J. Kunert, A. Drochner, J. Ott, H. Vogel, H. Fuess, Appl. Catal. A 269 (2004) 53–61.

[10] R. Boehling, A. Drochner, M. Fehlings, D. Koenig, H. Vogel, Chem. Eng. Technol. 22 (1999) 747–750.

[11] T. Roisnel, J. Rodriguez-Carvajal, Mater. Sci. Forum 378–381 (2001) 118–123.

[12] L.B. McCusker, R.B. von Dreele, D.E. Cox, D. Louër, P. Scardi, J. Appl. Cryst. 32 (1999) 36–50.

[13] V.L. Volkov, G.S. Tynkachva, A.A. Fotiev, E.V. Tkachenko, Russ. J. Inorg. Chem. 17 (1972) 1469–1470.

[14] I. Svoboda, personal communication.

[15] W. Freundlich, P. Pailleret, C.R. Hebd. Séances Acad. Sci. Paris 261 (1965) 153–155.

[16] E. Salje, R. Gehlig, K. Viswanathan, J. Solid State Chem. 25 (1978) 239–250.

[17] W. Freundlich, C.R. Hebd. Séances Acad. Sci. Paris 260 (1965) 3077–3079.

[18] Y. Hu, P.K. Davies, J. Solid State Chem. 105 (1993) 489–503.

[19] L.M. Plyasova, L.P. Soloveva, S.V. Tsybulya, G.N. Kryukova, V.A. Zabolotnyi, I.P. Olenkova, J. Struct. Chem. 32 (1991) 89–93.

[20] B. Gerand, G. Novogorocki, J. Guenot, M. Figlarz, J. Solid State Chem. 29 (1979) 429–434.

[21] G. Andersson, Acta Chem. Scand. 10 (1956) 623–628.

[22] F. Portemer, M. Sundberg, L. Kihlborg, M. Figlarz, J. Solid State Chem. 103 (1993) 403–414.

[23] R. Benchrifa, M. le Blanc, R. de Pape, Eur. J. Solid State Chem. 26 (1989) 593–601.

[24] A. Magneli, Ark. Kemi, Mineral. Geol. A 19 (1945) 1–14.

[25] F.R. Theobald, R. Cabala, J. Bernhard, J. Solid State Chem. 17 (1976) 431–438.

[26] G. Andersson, A. Magneli, Acta Chem. Scand. 4 (1950) 793–797.

[27] J.B. Parise, E.M. McCarron III, R.B. von Dreele, J.A. Goldstone, J. Solid State Chem. 93 (1991) 193–201.

[28] L. Kihlborg, Ark. Kemi 21 (1963) 357–364.

[29] L. Kihlborg, Ark. Kemi 21 (1963) 427–437.

[30] H.A. Eick, L. Kihlborg, Acta Chem. Scand. 20 (1966) 1658–1666.

[31] A.H. Adams, Structural Investigations on V-Mo-(W)-Mixed Oxide Materials for Oxidation Catalysis (in German), Shaker-Verlag, Aachen, 2004.

[32] F. Haaß, A.H. Adams, T. Buhrmester, G. Schimanke, M. Martin, H. Fuess, Phys. Chem. Chem. Phys. 5 (2003) 4317–4324.

[33] O. Ovsitser, Y. Uchida, G. Mestl, G. Weinberg, A. Blume, J. Jaeger, M. Dieterle, H. Hibst, R. Schloegl, J. Mol. Catal. A 185 (2002) 291–303.

[34] T. Ressler, O. Timpe, T. Neisius, J. Find, G. Mestl, M. Dieterle, R. Schloegl, J. Catal. 191 (2000) 75–85.

[35] T. Ressler, R.E. Jentoft, J. Wienhold, M.M. Guenter, O. Timpe, J. Phys. Chem. B 104 (2000) 6360–6370.

[36] T. Ressler, J. Wienhold, R.E. Jentoft, T. Neisius, J. Catal. 210 (2002) 67–83.

[37] S. Knobl, G.A. Zenkovets, G.N. Kryukova, O. Ovsitser, D. Niemeyer, R. Schloegl, G. Mestl, J. Catal. 215 (2003) 177–187.

[38] M. Dieterle, G. Mestl, J. Jaeger, Y. Uchida, H. Hibst, R. Schloegl, J. Mol. Catal. A 174 (2001) 169–185.